Nodal correlations in the incompressible composite fermion liquid

Kenneth L. Graham, Sudhansu S. Mandal,* and Jainendra K. Jain
Department of Physics, 104 Davey Laboratory, The Pennsylvania State University, University Park, Pennsylvania 16802
(Received 17 December 2002; published 5 June 2003)

To search for possible correlations in the system of interpenetrating liquids of zeroes and electrons in the fractional quantum Hall effect, this paper studies several ground state correlation functions involving particles and zeroes in the incompressible states of composite fermions at filling factors $\nu=2/5$, 3/7, and 4/9. It is found that the zeroes form a liquid of their own in which they repel one another at short distances, and also repel particles (with the obvious exception of the Pauli zeroes that are tied to the particles). For certain states, it is found that three body configurations containing two nearby electrons and a zero in the middle are highly probable, indicating that the zeroes tend to insert themselves between nearby particles in an effort to keep them apart.

DOI: 10.1103/PhysRevB.67.235302 PACS number(s): 73.43.−f, 71.10.Pm

I. INTRODUCTION

Sometimes the vortex structure of a wave function reveals important information about the underlying physics. An example is the ground state wave function of bosons in two dimensions, which is everywhere positive, that is, it contains no vortices. (A vortex is defined as a point a path around which has a phase change of 2π associated with it. For hard core bosons, the wave function will vanish for the configurations in which two bosons coincide, but still does not become negative.) For most states however, for example a superconductor or a Landau Fermi liquid, no significance has been attached to the nodal structure. (We note that we have in mind here the microscopic wave function. For a superconductor the nodes in the *order parameter* do have a physical significance.)

Vortices have played an important role in the theory of the fractional quantum Hall effect (FQHE)[1] because of certain special properties of the wave functions in the lowest Landau level (LLL). In the lowest Landau level, an exact statement can be made about the number of zeroes at a given filling factor. In the disk geometry, the single particle wave functions have the form $z^n e^{-|z|^2/4}$, where $z=x-iy$ denotes the coordinates of an electron as a complex number and the unit of length has been chosen to be the magnetic length, $l_0=\sqrt{\hbar c/eB}$. This state is a Gaussian localized within a circle of radius $\sqrt{2n}l_0$. For a disk of a finite radius $R=\sqrt{2n_{\max}}l_0$, all states with $n\leqslant n_{\max}$ are available for electrons. The filling factor ν is defined as the ratio of the number of electrons to the number of available single particle orbitals.

For N electrons at filling factor ν, the general wave function has the form

$$\Psi=F_A[\{z_j\}]\exp\left[-\frac{1}{4}\sum_l |z_l|^2\right], \tag{1}$$

where $F_A[\{z_j\}]$ is an antisymmetric polynomial of the coordinates. The important feature of the lowest Landau level physics is that the polynomial F is *analytic* in the z's; i.e., it does not depend on the complex conjugates z^*'s. This allows one to make an exact statement about the number of zeroes of the wave function. For this purpose, we view the wave function as the function of a single coordinate, say z_j, treating all other coordinates as fixed constants. For a given filling factor ν, there are N/ν single particle states occupied, implying that the largest power of z_j in the polynomial part of the wave function is N/ν, which, according to the fundamental theorem of algebra, is also the number of zeroes of the wave function. [Here, we have neglected O(1) corrections. For a finite system, the number of zeroes can of course be determined exactly for given boundary conditions.] We also note that a zero in the lowest Landau level is also a vortex, in that it produces a phase of -2π when z_j goes around it in a closed counterclockwise loop. However, for reasons explained in the next section, we will reserve the name ''vortex'' for a zero bound to a particle, and use the ''zeroes'' or ''nodes'' for the zeroes *not* bound to particles.

The role of vortices was apparent in Laughlin's wave function for the FQHE ground state at filling factor $\nu=1/m$, m being an odd integer,[2] given by

$$\Psi_{1/m}=\prod_{j<k}(z_j-z_k)^m\exp\left[-\frac{1}{4}\sum_l |z_l|^2\right]. \tag{2}$$

This wave function has a remarkably simple nodal structure. If you fix all particles except one, the only times the wave function vanishes is when the mobile particle hits another particle. Each particle sees a zero (in fact an mth order zero) at every other particle and nowhere else. Laughlin's wave function thus contains no free zeroes.[3]

The Pauli principle guarantees that each electron has at least one vortex bound to it. However, in general, electrons can bind any odd number of vortices. At $\nu=1/m$, there are m zeroes per electron which are taken to be all bound to electrons in Laughlin's wave function. That is not possible at other fractions. Consider for example $\nu=2/5$, for which there are 2.5 zeroes per particle. There is exactly one zero bound to each electron, with the other 1.5 zeroes away from electrons. The observation of FQHE at numerous filling factors not of the form $\nu=1/m$ demonstrates that the ''no-free-zeroes property'' at $\nu=1/m$, which leads to a simple wave function at $\nu=1/m$, is not essential for the FQHE. (Even at $\nu=1/m$, there is, strictly speaking, only one zero on each electron in the *true* ground state. But the other $m-1$ zeroes

are very close to the particle positions, and $\Psi_{1/m}$ makes the approximation of putting them all on particles.) We will see that Laughlin's wave function is an untypical case; it has little bearing on the configuration of zeroes of general incompressible states.

Vortices also play a fundamental role in the wave functions for the general FQHE states, written by one of us:[4]

$$\Psi_{n/(2np+1)}=\prod_{j<k}(z_j-z_k)^{2p}\Phi_n, \tag{3}$$

where Φ_n is the wave function for n fully occupied Landau levels. This wave function has the following interpretation. Due to the presence of the Jastrow factor $\Pi_{j<k}(z_j-z_k)^{2p}$ there are an even number $(2p)$ of vortices bound to each electron. The bound state is interpreted as a particle, called the composite fermion. The crucial consequence of the formation of composite fermions is that they experience a reduced effective magnetic field $B^*=B-2p\rho\phi_0$, where ρ is the two-dimensional density of electrons and $\phi_0=hc/e$ is the flux quantum. The origin of the effective magnetic field is a direct consequence of the formation of composite fermions through binding of electrons and vortices, which can be seen as follows. Imagine taking one particle in a loop enclosing an area A and asking what is the associated phase. In addition to the usual Aharonov-Bohm phase $2\pi BA/\phi_0$, there is also a contribution from the vortices bound to composite fermions. There are on average ρA particles inside the loop, each carrying $2p$ vortices, and each vortex produces a phase of -2π, giving a contribution of $-2\pi 2p\rho A$. When added to the Aharonov-Bohm phase, the total phase can be interpreted as the Aharonov-Bohm phase coming from an effective magnetic field B^*. In short, the phases due to the bound vortices partly cancel the Aharonov-Bohm phase to make it seem as though the particles were moving in a reduced effective magnetic field.

The wave function $\Psi_{n/(2n+1)}$ has more zeroes than those counted above (N/ν), because it does not reside strictly in the lowest Landau level. Φ_n involves higher Landau levels and is not analytic. The Jastrow factor provides two vortices per particle, while Φ_n, which is not analytic, contains both nodes and antinodes, the number of which is not fixed but depends on the configuration of particles. It provides one additional zero, either a node or an antinode, on each particle to restore antisymmetry.

In the limit of very large magnetic fields, when the Landau level spacing is large compared to the interaction energy, the wave functions in Eq. (3) must be projected onto the lowest electronic Landau level to produce physically useful wave functions. Upon projection, one of the two bound zeroes must move off of the particles, and the antinodes in Φ_n are annihilated by combining with nodes. No longer are two vortices explicitly bound to electrons, and the efforts to see composite fermions directly in a lowest Landau level theory have proved largely unsuccessful for this reason; in fact, the composite fermion physics will appear rather mysterious to someone who refuses to use higher Landau levels at an intermediate step. If someone were to give us the the lowest Landau level wave function (obtained, say, in exact diagonalization studies), it would be impossible to deduce from it that it can be obtained by the lowest Landau level projection of the product wave function given in Eq. (3). (The composite fermion physics was originally motivated by the empirical similarity between the fractional and the integral quantum Hall effects.)

It is worth stressing that this is not an objection against composite fermions. In physics problems, there is a range of parameters for which the Hamiltonian describes the qualitative physics of interest. It is obviously unrealistic to demand a solution for every possible choice of variables. The usual approach is to identify (at least) one point in this parameter space of the Hamiltonian where the physics is transparent, which also correctly describes the physics of the adiabatically connected ''physical'' point, and then proceed to obtain quantitative information perturbatively. The wave functions in the lowest Landau level are rather complicated and do not directly lend themselves to a simple interpretation. The nontrivial accomplishment of the composite fermion (CF) theory is to show that they are adiabatically connected, through lowest Landau level projection, to the remarkably simple wave functions given in Eq. (3), from which the essential physics can be read off. Both the qualitative composite fermion physics, encoded in the effective magnetic field, and the quantitative validity of the wave functions have been confirmed in numerous experimental and theoretical studies in the lowest Landau level.[5]

Nonetheless the issue of the nodal structure of the FQHE states restricted to the lowest Landau level remains of interest. Can we make any sharp statements regarding the nodes of general FQHE states? Does one node remain close to each particle? Can some kind of bound state of electrons and zeroes be identified in the lowest Landau level wave function?

The zeroes have been studied in the past for a single electron in a disorder potential.[6] They have also been determined for many electron systems with fairly small N for a few random configurations of particles.[7] However, random configurations are often highly improbable, and also just a few snapshots may not give us much useful information. In this paper, we calculate the ground state averages of certain correlation functions involving particles and zeroes in a systematic study at several fillings of the lowest Landau level ($\nu=2/5$, 3/7, and 4/9). The correlation functions are calculated by Monte Carlo, with probable configurations generated according to the Metropolis algorithm.

A useful first step is to study pair-distribution functions for either two zeroes or one particle and one zero. The former $g_{zz}(r)$ gives the probability of finding two zeroes at a distance r, and the latter g_{pz} gives the probability of finding a particle and a zero at a distance r. We find that just as electrons, the zeroes form a liquid with short distance correlations. We then proceed to study a correlation function involving *two* particles and a zero $g_{ppz}(d,\mathbf{r})$, which gives the nodal density as a function of the position $\mathbf{r}$, with two particles held fixed at $(d/2,0)$ and $(-d/2,0)$. This correlation function reveals that, for $\nu=2/5$, zeroes tend to place themselves with high probability right in the middle of nearby pairs of particles, but such correlations weaken as more levels of composite fermions are filled (e.g., for $\nu=4/9$).

It ought to be emphasized that the intention of this study is look for correlations inside the CF fluid to gain further insight into its physics, and not to provide a new interpretation for composite fermions. We work with the lowest Landau level projections of the wave functions of Eq. (3), which are known to be accurate representations of the exact lowest Landau level wave functions.

The plan of the paper is as follows. We begin by discussing an important distinction between the on-particle and off-particle zeroes of the wave function. Section III contains the calculational details, including the wave functions, the definitions of the correlation functions, and the method for finding zeroes. Section IV contains results for the various correlation functions involving zeroes and particles. The paper is concluded in Sec. V.

II. NODES VERSUS VORTICES

What principle determines the configuration of the zeroes? Undoubtedly, the zeroes distribute themselves, to the extent allowed by general constraints of the Pauli principle and angular momentum conservation, so as to allow maximum repulsion between electrons.

It may appear at first sight that electrons and zeroes attract one another, based on the argument that a positive charge may be associated with a zero, due to the fact that electrons avoid it exposing the positively charged background. Let us first discuss the charge of a zero. Here, following Ref. 8, we find it important to make a distinction between zeroes which are on or off the particles. A vortex in the wave function at η is created by multiplication by the factor $\Pi_j(z_j-\eta)$, which ensures that *all* electrons avoid η. It clearly has a charge deficiency associated with it. The off-particle zeroes of a given particle are not the zeroes of other particles (this can be explicitly seen in Fig. 1, which shows the positions of the zeroes of all particles for a given starting configuration), and therefore are not avoided by all particles. No charge deficiency is necessarily associated with the off-particle zeroes of a given particle, so they are not vortices in any real sense. The zero bound to a particle behaves differently. It is a zero for *all* particles (except, of course, the particle to which it is bound). The on-particle zero creates a correlation hole around the particle, which has a positive charge associated with it. We will reserve the use of the term vortex for the on-particle zeroes, such as the ones that arise from the Jastrow factors in Eqs. (2) and (3). The off-particle zeroes, which do not have a direct physical significance, will be called either nodes or simply zeroes.

How about the attraction between zeroes and particles? Consider the zeroes of a test particle. By definition, the zeroes are where the test particle is not, which implies a repulsion between a particle and its zeroes. One may ask if there may be some attraction between the zeroes of the test particle and *other* particles. Such an attraction is not analogous to the attraction between two oppositely charged objects, but can possibly be induced by the fact that the zeroes of the test particle repel it, so having them close to the other particles will ensure that the test particle avoids them as well. The reality, in general, is much more complex than this simple-minded single-particle argument might suggest, because the zeroes in the wave function are distributed so as to ensure that *all* particles optimally avoid one another, not just the test particle. In the case of $\nu=1/m$, the zeroes of the test particle sit on other particles because such a binding is allowed by Pauli principle, and also guarantees repulsion between *all* pairs. Unfortunately, for other filling factors the situation is not so simple. The only sure way to answer this question is by actually calculating various correlation functions involving zeroes and particles.

It may also be noted in this context that the zeroes do not have their own independent dynamics. The positions of the zeroes are completely fixed once the positions of the particles are fixed. [The wave functions in Eq. (3) have no parameters other than the particle positions.] When calculating various physical quantities, for example the current, only the particles ought to be considered. We discussed above how the off-particle zeroes do not have a well-defined charge associated with them. Consider then, the on-particle zeroes, which are vortices and produce a positively charged correlation hole around each particle. They cannot contribute to the current, despite their associated correlation hole, because the positively charged background is static.

III. CALCULATIONAL METHOD

A. Wave functions

Our calculations were performed in the standard spherical geometry,[9,10] where N electrons lie on the surface of a sphere under the influence of a radial magnetic field corresponding to total flux $2Qhc/e$ produced by a magnetic monopole at the sphere's center. The monopole charge Q may be an integer or half-integer, in accordance with Dirac's quantization condition. This allows us to map the problem of N strongly interacting electrons at flux $2Q$ into N weakly interacting CF's at flux $2q=2Q-2p(N-1)$. The wave function for interacting electrons has the standard form[4,11]

$$\Psi_Q=\mathcal{P}_{\rm LLL}\Phi_1^{2p}\Phi_q, \tag{4}$$

where Φ_1 describes the fully filled lowest Landau level and Φ_q represents Slater determinant wave functions of noninteracting electrons at q. The single-particle basis states that constitute Φ_q are the monopole harmonics[10]

$$Y_{q,n,m}(\Omega_j)=N_{q,n,m}(-1)^{q+n+m}e^{iq\phi_j}u_j^{q-m}v_j^{q+m}\sum_{s=0}^{n}(-1)^s \times\binom{n}{s}\binom{2q+n}{q+n+m-s}(v_j^*v_j)^{n-s}(u_j^*u_j)^s, \tag{5}$$

where $n=0,1,\ldots,$ is the Landau level index, $m=-l,-l+1,\ldots,l-1,l$ labels the degenerate states in the nth LL, and $l=q+n$. The normalization coefficient is given by

$$N_{q,n,m}=\left(\frac{(2q+2n+1)(q+n+m)!(q+n-m)!}{4\pi n!(2q+n)!}\right)^{1/2}. \tag{6}$$

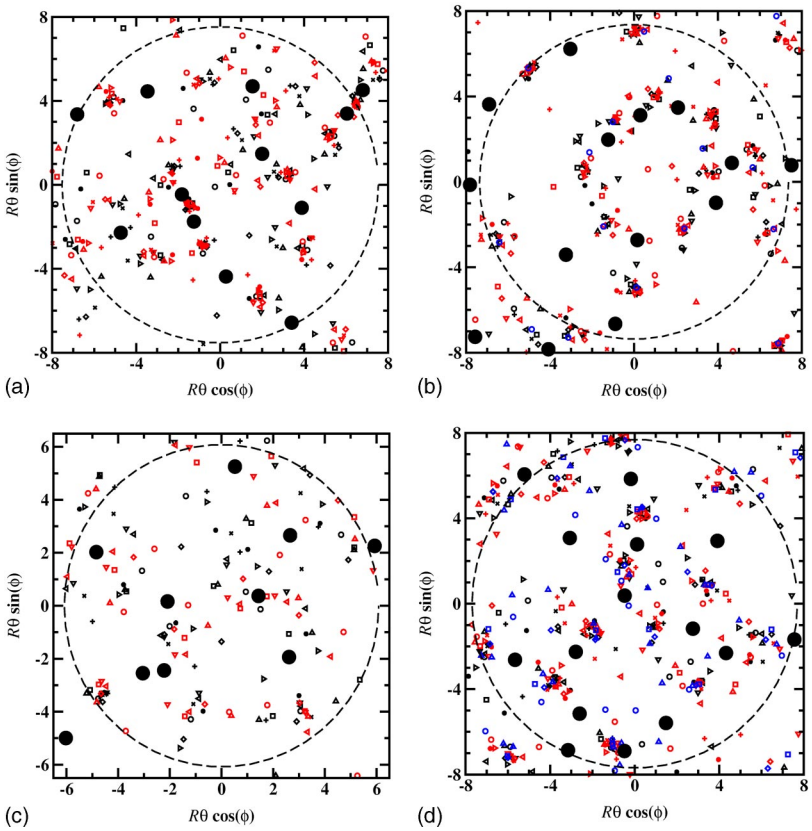

FIG. 1. Positions of the zeroes of all particles. The four panels correspond, from (a) to (d), to (a) $\nu=2/5$, (b) 3/7, (c) 4/9, and (d) 5/11 for $N=20$, 21, 16, and 25 particles, respectively. The particle positions are shown with large, filled circles, and the zeroes with unfilled symbols. The zeroes are determined by moving one particle while holding the others fixed at the positions shown. Different symbols are used for the zeroes of different particles. The sphere is plotted in polar coordinates. The north pole is the origin; with the arc length $R\theta$ used as the radius and the azimuthal coordinate ϕ as the polar angle. The equator is given by the dashed line. Distance is measured in units of the magnetic length l_0. One must be mindful of distortions in the distances while depicting the spherical geometry in a plane, as one goes farther from the north pole. For that reason, the figure does not extend much beyond the equator; the particles and zeroes closer to the south pole are not shown. (Of course, all of the zeroes were calculated.)

Ω_j represents the position of the jth electron on the surface of the unit sphere, and

$$u_j \equiv \cos(\theta_j/2)\exp(-i\phi_j/2), \tag{7}$$

$$v_j \equiv \sin(\theta_j/2)\exp(i\phi_j/2). \tag{8}$$

The wave function Φ_q is the constructed as a Slater determinant of the monopole harmonics

$$\mathrm{Det}[Y_i(\Omega_j)]. \tag{9}$$

It has previously been shown that the process of multiplying Φ_q by Φ_1^2 and then projecting into the LLL gives[11]

$$\mathcal{J}\mathrm{Det}[\overline{Y}_i(\Omega_j)], \tag{10}$$

in which $\overline{Y}_{q,n,m}$ and $\mathcal{J}$ are defined as

$$\begin{aligned}\overline{Y}_{q,n,m}(\Omega_j) = &\left[\frac{[2q+p(N-1)+1]!}{[2q+p(N-1)+n+1]!}\right] \\ &\times N_{q,n,m}(-1)^{q+n+m}u_j^{q+m}v_j^{q-m} \\ &\times\sum_{s=0}^{n}(-1)^s\binom{n}{s}\binom{2q+n}{q+n-m-s} \\ &\times u_j^s v_j^{n-s}[\overline{U}_j^s\cdot\overline{V}_j^{n-s}\cdot 1],\end{aligned} \tag{11}$$

where

$$\overline{U}_j \equiv p\sum_k{}' \frac{v_k}{u_j v_k - v_j u_k} + \frac{\partial}{\partial u_j}, \tag{12}$$

$$\overline{V}_j \equiv p\sum_k{}' \frac{-u_k}{u_j v_k - v_j u_k} + \frac{\partial}{\partial v_j}, \tag{13}$$

and

$$\mathcal{J} \equiv \prod_{j,k\neq j}(u_j v_k - v_j u_k)^p \exp\left(\frac{ip}{2}(\phi_j+\phi_k)\right). \tag{14}$$

B. Correlation functions

We calculate the pair-distribution functions of zeroes $g_{zz}(r)$, particle-zero pairs $g_{pz}(r)$, particle-off-particle zero pairs $g_{p\bar{z}}(r)$, and the three-point correlation function $g_{ppz}(d,\mathbf{r})$, by the Monte Carlo method (with Metropolis algorithm) in the spherical geometry,[9] all properly normalized to approach unity at large r.

To illustrate the method, easily generalized to other correlation functions, we begin by discussing the two-point correlation function

$$\begin{aligned}g_{pp}(\mathbf{r}_1,\mathbf{r}_2) = &\frac{N(N-1)}{\rho_0^2}\int\cdots\int d^2r_3\cdots d^2r_N \\ &\times|\Psi(\mathbf{r}_1,\ldots,\mathbf{r}_N)|^2,\end{aligned} \tag{15}$$

which, for a homogeneous system, depends only on $|\mathbf{r}_1-\mathbf{r}_2|$, where the $\mathbf{r}_i$ are the positions of indistinguishable par-

ticles. (Here we stress the indistinguishability because the normalization factors change if one calculates correlations between distinguishable entities. More discussion will follow below.) Since the ground state is homogeneous, one can define the pair correlation function as

$$g_{pp}(\mathbf{r}) = \frac{1}{A}\int d^2R\, g(\mathbf{r},\mathbf{R}), \tag{16}$$

where $\mathbf{r}=\mathbf{r}_1-\mathbf{r}_2$ is the distance between the pair of particles (or zeroes) and $\mathbf{R}=(\mathbf{r}_1+\mathbf{r}_2)/2$ is the pair's center of mass. Since the system is isotropic, the pair correlation function depends only on $r\equiv|\mathbf{r}|$:

$$g_{pp}(r) = \frac{1}{\rho_0 N}\left\langle \sum_{i\neq j} \delta(\mathbf{r}-\mathbf{r}_i+\mathbf{r}_j)\right\rangle. \tag{17}$$

We evaluate the pair-distribution function using the Monte Carlo method, generating configurations according to the Metropolis algorithm and determining the distances between *all* pairs for each configuration. The brackets $\langle\rangle$ in Eq. (17) denote both angular and ground state averaging. On the sphere, after sectioning the surface of the sphere into bins of sufficiently small area (more on this later), Eq. (17) may be represented in a form useful for the Monte Carlo method:

$$g_{pp}(r) = \frac{1}{N_{\mathrm{MC}}\rho_0 N}\sum_{k=1}^{N_{\mathrm{MC}}} \frac{\sum_{i\neq j=1}^{N} \Theta(r_{ij}^{(k)}-r)}{a_r}, \tag{18}$$

where $\Theta(r_{ij}^{(k)}-r)$ is 1 or 0 depending on whether the distance between the pair ij lies inside or outside the bin containing r, a_r is the area of the bin, and N_{MC} is the total number of Monte Carlo steps.

The preceding equation can be modified straightforwardly for g_{zz} and g_{pz}:

$$g_{zz}(r) = \frac{1}{N_{\mathrm{MC}}\rho_Z N_Z}\sum_{k=1}^{N_{\mathrm{MC}}} \frac{\sum_{i\neq j=1}^{N_Z} \Theta(r_{ij}^{(k)}-r)}{a_r}, \tag{19}$$

$$g_{pz}(r) = \frac{1}{2N_{\mathrm{MC}}\rho_0 N_Z}\sum_{k=1}^{N_{\mathrm{MC}}} \frac{\sum_{i=1}^{N}\sum_{j=1}^{N_Z} \Theta(r_{ij}^{(k)}-r)}{a_r}, \tag{20}$$

where N_Z is the number of zeroes, and ρ_Z is their density. Equation (20) may also be used to calculate $g_{p\bar{z}}(r)$ if N_Z is replaced by the number of off-particle zeroes $N_{\bar{Z}}=N_Z-N+1$.

Note the factor of 1/2 in Eq. (20). Such unconventional normalization factors will appear when calculating correlations between distinguishable entities, for example a particle and a zero. Usually, the normalization factor of an n-point correlation function of identical ''particles'' is the number of n-tuples that can be chosen from N particles. The counting is slightly more complicated for distinguishable ''particles,'' where we must calculate some (m,n)-point correlation function, choosing m particles of type A from a possible M and n type B particles from a possible N (assume $M\geqslant N$). The normalization factor will then be the number of permutations of m type A particles and n type B particles.

The three-point correlation function

$$g_{ppz}(d,\mathbf{r}) = \frac{1}{\rho_Z}\rho'(\mathbf{r}) \tag{21}$$

is evaluated by determining $\rho'(\mathbf{r})$, the density of zeroes at $\mathbf{r}$, with the constraint, indicated by the prime, that two composite fermions are held fixed at $(\pm d/2,0)$. This constraint is easily incorporated into the Monte Carlo algorithm. In the spherical geometry, the fixed particles are positioned at $(\theta_1,\phi_1)=(d/2R,0)$ and $(\theta_2,\phi_2)=(d/2R,\pi)$. Eq. (21) can also be recast in a form convenient for Monte Carlo calculations

$$g_{ppz}(d,\mathbf{r}) = \frac{1}{N_{\mathrm{MC}}\rho_z}\sum_{j=1}^{N_{\mathrm{MC}}} \frac{\sum_{i=1}^{N_Z} \Theta(\mathbf{r}_i^{(j)}-\mathbf{r})}{a_{\mathbf{r}}}, \tag{22}$$

where $\Theta(\mathbf{r}_i^{(j)}-\mathbf{r})$ is 1 or 0 depending on whether the ith zero lies inside or outside the bin containing $\mathbf{r}$.

C. Binning the sphere

Significant care must be exercised in binning the sphere. We give here some of the relevant details of our method.

Since the pair-distribution functions depend only on r, the surface of the sphere can be divided into infinitesimal spherical frusta. We measure distance between pair ij as chord length $r_{ij}=2R|u_iv_j-v_iu_j|$; corresponding to the pair lying in the bin indexed by $1+(\text{integer part})(Dr_{ij}/2R)$, where D is the number of bins. The mth bin, at distance $2R(m-1/2)/D$, has area

$$\frac{4\pi R^2(m-1/2)}{D}\left|\sin^{-1}\left(\frac{m}{D}\right)-\sin^{-1}\left(\frac{m-1}{D}\right)\right| \times\sqrt{1-\left(\frac{(m-1/2)}{D}\right)^2},$$

where $m=1,\ldots,D$. We have used $D=200$.

For g_{ppz}, which depends on θ and ϕ, binning is slightly more complicated. Since we are primarily interested in the behavior of g_{ppz} near the fixed particles, smaller bins are chosen here to capture finer details. The ϕ bins are generated according to $\phi_m=2\pi m/D$, with $m=1,\ldots,D$. The θ arc from 0 to π, however, is binned into three regions. The first region covers $\theta\epsilon(0,\pi/A_1]$ and is given by $\theta_n=\pi n/A_1D_1$, where $n=1,\ldots,D_1$ and $A_1=(\text{integer part})(\pi/2\theta_1)+1$. This choice of A_1 allows the fixed particles to lie in the middle of region one. The second region covers $\theta\epsilon(\pi/A_1,\pi/A_2]$ and is given by $\theta_n=\pi n/A_3D_2+\pi/A_1$, where $A_2=2$, $A_3=(A_1-A_2)/(A_1A_2)$, and $n=1,\ldots,D_2$. While we have selected $A_2=2$, it is essentially a free parameter, provided $A_1>A_2$. Region three covers $\theta\epsilon(\pi/A_2,\pi/A4]$ and is given by $\theta_n=\pi n/A_5D_3+\pi/A_2$, where $A_4=1$, $A_5=(A_2-A_4)/(A_2A_4)$, and $n=1,\ldots,D_3$. We have selected $A_4=1$, though it's only constrained to be

less than A_2. In particular we have chosen $D=200$, $D_1=D_2=80$, and $D_3=40$ (note that $D_1+D_2+D_3=D$); a large D_1 allows high resolution near the fixed particles. The bin area $a_{\mathbf{r}}$ is given by $2\pi R^2 \sin(\theta_n)\delta\theta_n/D$, where $\delta\theta_n=\theta_n-\theta_{n-1}$ and θ_n lies in the appropriate region.

D. Finding zeroes

We find the zeroes by minimizing the modulus of the wave function in a two-dimensional subspace. There are several minimization methods to choose from, some fast, others robust. Since the wave function has many zeroes we must use a method that easily finds local minima, and since the wave function is a Slater determinant, calculates the wave function as few times as possible. Slater determinant calculation is costly because each single-CF basis state depends on the coordinates of all N electrons. As a result we cannot use standard $\mathcal{O}(N)$ updating techniques for fermions[12] to calculate the determinant and $\mathcal{O}(N^3)$ operations are needed instead at each Monte Carlo iteration. Projecting onto the lowest Landau level is also increasingly costly as we consider more CF-LL's since, for the FQH state at $\nu=n/|2pn\pm1|$, the cost of projection goes as n^3.[3,11] Thus the computation time scales as

$$T\propto N^3 n^3 N_{\mathrm{MC}} S N_{\mathrm{WF}}, \tag{23}$$

where N_{WF} is the average number of wave function calculations needed to find a single zero and S is the number of zeroes. These considerations rule out methods such as conjugate gradient. Instead, we use a two-dimensional Newton-Raphson method.

The Newton-Raphson method is a three-step process, the first of which is testing whether or not the initial guess is a zero. If the initial point is a zero then you stop and move on to the next guess; if the point is not a zero then take steps in the direction of steepest descent until a zero is found. Steps are computed by first assuming that the guess is close to the zero, which allows one to Taylor expand the modulus of the wave function about the zero. All particles except the Nth are fixed, so we expand in the coordinates (θ,ϕ) of the trial point (the Nth particle)

$$f(\theta+d\theta,\phi+d\phi)=f(\theta,\phi)+\left.\frac{\partial f}{\partial\theta}\right|_{(\theta,\phi)} d\theta+\left.\frac{\partial f}{\partial\phi}\right|_{(\theta,\phi)} d\phi\equiv 0,$$

where $f(\theta,\phi)=|\Psi(\theta,\phi)|$ and $(\theta+d\theta,\phi+d\phi)$ is the position of the new point. Since the step must be in the direction of steepest descent, $(-\nabla|\Psi|)$ must be parallel to the Newton step. Thus the Newton step is given by

$$d\theta=\frac{-f(\theta,\phi)\left.\frac{\partial f}{\partial\theta}\right|_{(\theta,\phi)}}{(|\nabla f|_{(\theta,\phi)})^2} \tag{24}$$

and

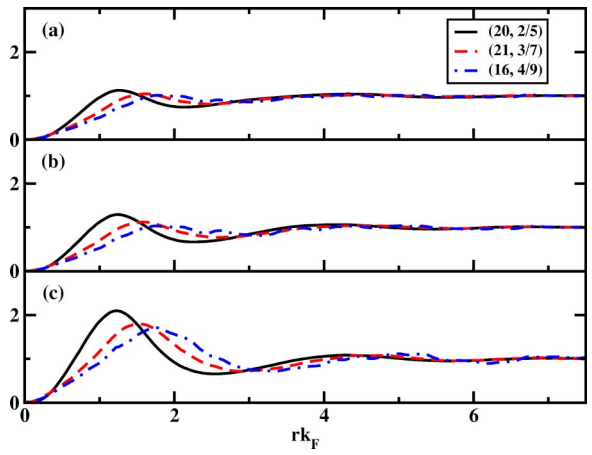

FIG. 2. Pair-distribution functions for three FQHE states at $\nu=n/(2n+1)$, corresponding to n filled Landau levels of composite fermions. $N=20$, 21, and 16 particles have been used for $n=2$, 3, and 4, respectively. (a), (b), and (c) show the probability of having two zeroes, a particle and a zero, and a particle and an off-particle zero, respectively, at a distance r. Following Ref. 14, we choose the unit of length for this plot as $k_F^{-1}=(4\pi\rho)^{-1/2}$.

$$d\phi=\frac{-f(\theta,\phi)\left.\frac{\partial f}{\partial\phi}\right|_{(\theta,\phi)}}{\sin^2(\theta)(|\nabla f|_{(\theta,\phi)})^2}. \tag{25}$$

Typically, a sequence of Newton steps will quickly converge to a zero, provided the guess lies reasonably close. If the Monte Carlo step size is sufficiently small, the zeroes will move only slightly from their previous positions, allowing the zeroes of the previous configuration to be guesses for the current configuration. Since a very small step size is not optimal for Metropolis algorithm, we slightly move *all* particles relative to the average interparticle separation (rather than a single particle by a large step) with an acceptance ratio $\geqslant 75\%$. It is important, however, to realize that the comparative ease (and speed) of finding zeroes depends primarily on the configuration of particles and how much a configuration changes between Monte Carlo steps. Thus a somewhat uniformly distributed collection of particles more easily lends itself to such methods. Typically, we have performed calculations on systems containing up to 20 particles. For example, a calculation of g_{ppz} of the $\nu=2/5$ state for 20 particles with 50 000 Monte Carlo steps takes ~ 50 CPU h on our workstation (Digital Model 600au, Alpha CPU, 500 MHz). A similar calculation of 21 particles in the $\nu=3/7$ state takes ~ 67 CPU h on the same machine.

The only problem we have encountered with Newton-Raphson lies in the complexity of the basins of attraction. In Newton's method, for any polynomial with three or more distinct roots, the basins of attraction have disjointed *fractal* regions,[13] and nearby points can converge to far away zeroes. This has generally resulted in a given zero being found more than once, although a guess would sometimes fall into a periodic cycle, never converging to a root within the maximum number of Newton steps (up to five hundred). When this happens we obtain guesses by blanketing the sphere's

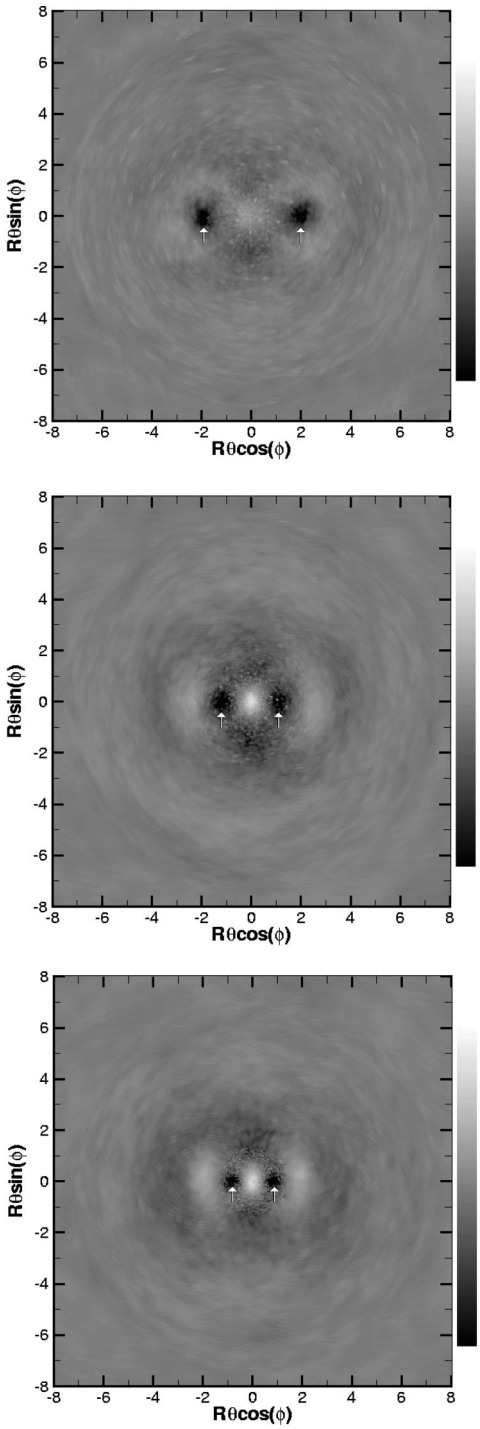

FIG. 3. g_{ppz} for 20 particles at $\nu=2/5$, with $d=1.0r_{pp}$, $0.5r_{pp}$, and $0.35r_{pp}$, where $r_{pp}=4l_0$, l_0 being the magnetic length. The sphere is plotted in polar coordinates. The north pole is the origin; with the arc length $R\theta$ used as the radius and the azimuthal coordinate ϕ as the polar angle. The white arrows represent the positions of the two fixed particles. The contours are shaded as follows. Black represents zero probability per unit area, the shade of grey toward the edges is a probability per unit area of one, with lighter shades representing probability per unit area greater than one, white being highest. Distance is measured in units of l_0.

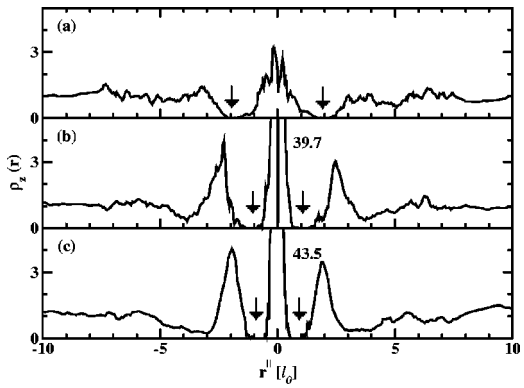

FIG. 4. Cross section of g_{ppz}, for 20 particles at $\nu=2/5$, along the arc passing through the fixed particle positions. In this and subsequent figures, the origin is the north pole and the fixed particle positions are represented by arrows. (a)–(c) correspond to $d=1.0r_{pp}$, $0.5r_{pp}$, and $0.35r_{pp}$, respectively. The numbers appearing next to the central peaks in (b) and (c) give the height of the peak.

surface with small plaquettes and examining the way the wave function changes sign as one moves around the edge of the plaquette. If both the real and imaginary parts of the wave function change sign twice as we move around the plaquette, then the plaquette's center is taken as a guess. Since these trial zeroes go into the Newton-Raphson method, in some rare occasions all zeroes are still not found; we completely ignore such a Monte Carlo iteration and return to the previous configuration, using its zeroes as input for the sums in the correlation functions. This is akin to the way a rejected Monte Carlo step is handled in the Metropolis algorithm.

A primary concern of any minimization method is the termination condition. For our purposes it is sufficient to require the modulus of the wave function to be below some maximal tolerance. Since there are trivial zeroes bound to each particle it is advantageous to use the modulus of the wave function near them to define the tolerance. We calculate the modulus of the wave function at some δ away from each of the first $N-1$ particles, using the lowest value as the

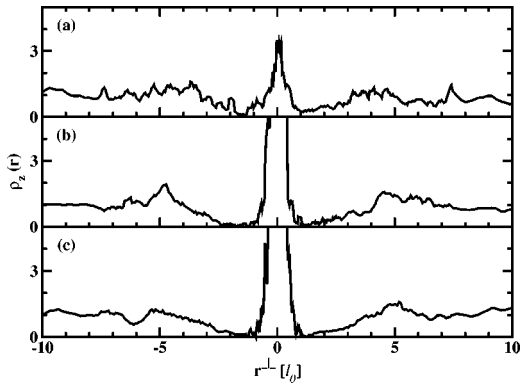

FIG. 5. Cross section of g_{ppz} for 20 particles at $\nu=2/5$, along the arc passing through the origin in a direction perpendicular to the arc joining the fixed particle positions. (a)–(c) correspond to $d=1.0r_{pp}$, $0.5r_{pp}$, and $0.35r_{pp}$, respectively.

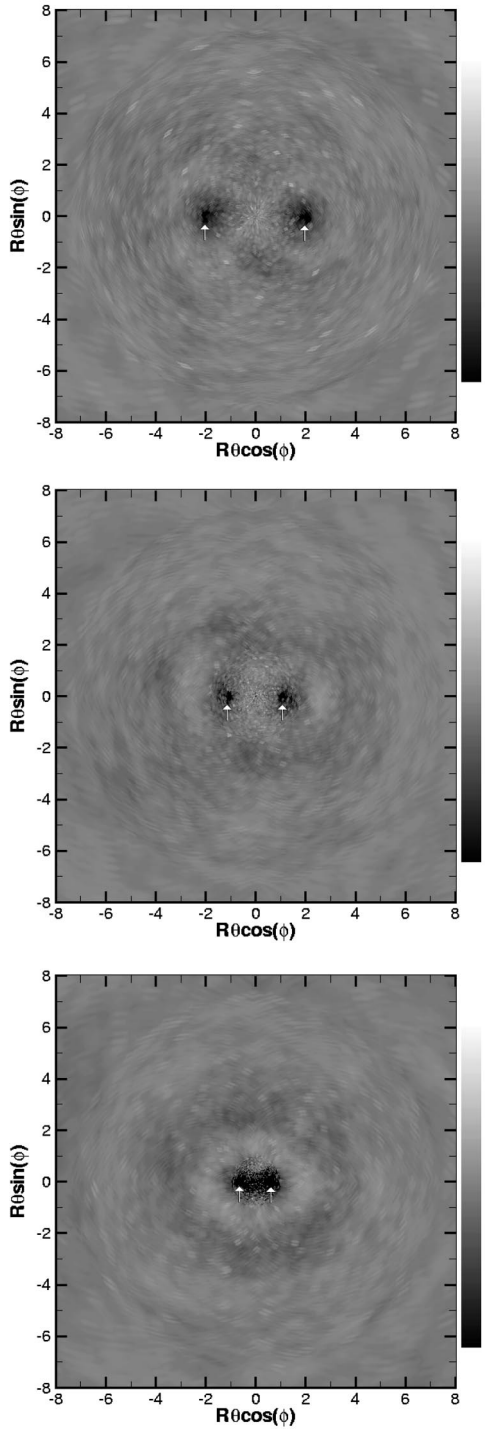

FIG. 6. g_{ppz} for 21 particles at $\nu=3/7$, with $d=1.0r_{pp}$, $0.5r_{pp}$, and $0.25r_{pp}$.

tolerance. As the particles move during Monte Carlo, what is or is not a good tolerance may change. To account for this, we recalculate the tolerance during each accepted Monte Carlo step. The shift δ indirectly determines the precison of the zeroes found from the Newton-Raphson method and needs be no smaller than the smallest bin size used to calculate the correlation functions. We use $\delta=10^{-3}l_0$ and are able to consistently resolve the position of the zero to at least four decimal places.

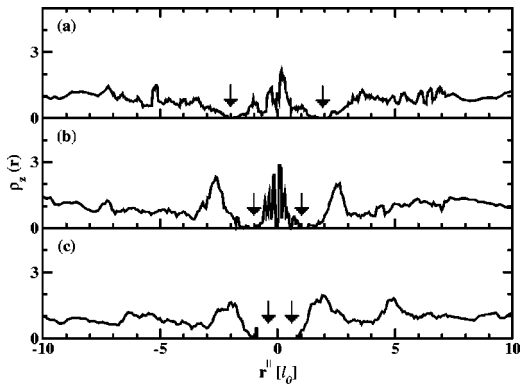

FIG. 7. Cross section of g_{ppz}, for 21 particles at $\nu=3/7$, along the arc passing through the fixed particle positions. (a)–(c) correspond to $d=1.0r_{pp}$, $0.5r_{pp}$, and $0.25r_{pp}$, respectively.

IV. CORRELATION FUNCTIONS

We have calculated several pair-distribution functions involving zeroes at filling factors $\nu=2/5$, 3/7, and 4/9. We now show the results and discuss what they signify. The particle-particle pair correlation function at these filling factors has been presented earlier.[14]

A. Zero zero

Figure 2(a) shows the zero-zero distribution function $g_{zz}(r)$ which gives the probability of finding two zeroes at a distance r. It approaches unity at long distances, indicating that the zeroes themselves form a liquid. At short distances, the zeroes avoid one another.

B. Particle zero

Figure 2(b) shows $g_{pz}(r)$, the probability of finding a zero at a distance r from a particle. The delta function at the origin, due to the single zero at the particle, is not shown explicitly. While forming their own liquid, the off-particle zeroes avoid particles. In fact, a repulsion between zeroes also guarantees a repulsion between the zeroes and particles, for the particles carry zeroes with them.

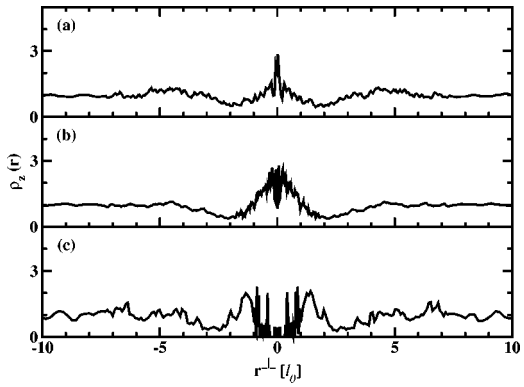

FIG. 8. Cross section of g_{ppz}, for 21 particles at $\nu=3/7$, along the arc passing through the origin in a direction transverse to the arc joining the fixed particle positions. (a)–(c) correspond to $d=1.0r_{pp}$, $0.5r_{pp}$, and $0.25r_{pp}$, respectively.

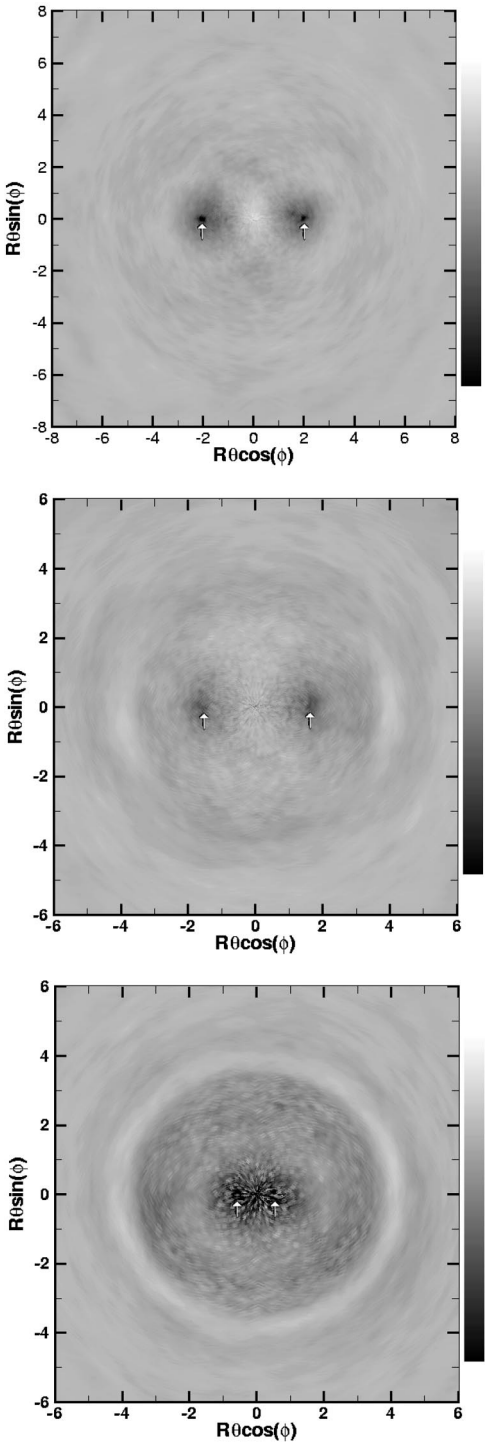

FIG. 9. g_{ppz} for 20 particles at $\nu=4/9$, with $d=1.0r_{pp}$, $0.5r_{pp}$, and $0.25r_{pp}$.

We also plot $g_{p\bar{z}}(r)$, the probability of finding an off-particle zero at a distance r from an on-particle zero, in Fig. (2(c). (This is the same as the correlation function for a particle and an off-particle zero.) Note that the curves are normalized differently. The close similarity between the three-plots demonstrates that the on-particle zeroes and the off-particle zeroes behave equivalently in the liquid of zeroes.

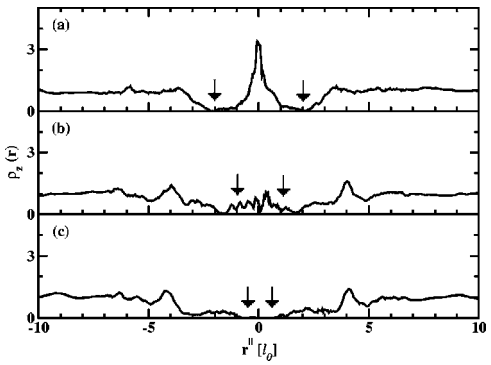

FIG. 10. Cross section of g_{ppz}, for 20 particles at $\nu=4/9$, along the arc passing through the fixed particle positions. (a)–(c) correspond to $d=1.0r_{pp}$, $0.5r_{pp}$, and $0.25r_{pp}$, respectively.

C. Particle-particle-zero (PPZ)

In Fig. 1, especially in the first two panels, the zeroes tend to locate themselves preferentially *between* pairs of particles, especially if the particles are closer than the typical interparticle separation. There is a bunching of the zeroes of various particles right in between pairs. This has motivated us to look at the correlations between a pair of particles and the zeroes. For this purpose, we hold two particles at a fixed distance d and calculate the probability of finding a zero in the neighborhood. Sufficiently far away, as expected, the probability of a zero is independent of the distance between the two fixed particles. We measure d in units of $4l_0$, roughly equal to the interparticle separation, which we call r_{pp}.

Figure 3 shows how the probability of finding a zero near the fixed particles evolves as d is varied from $1.0r_{pp}$ to $0.35r_{pp}$, for 20 particles at $\nu=2/5$. When the two fixed particles are at the typical interparticle separation, the particle-particle-zero correlation function is essentially the sum of two independent particle-zero correlation functions. When $d=1.0r_{pp}$, in top panel of Fig. 3, we see that finding a zero half-way between the fixed particles is roughly as likely as finding a zero far away. As d is decreased to $r_{pp}/2$ and $0.35r_{pp}$, respectively, the probability of finding a zero half-way between the fixed particles increases by more than an order of magnitude. As the fixed particles are pushed to-

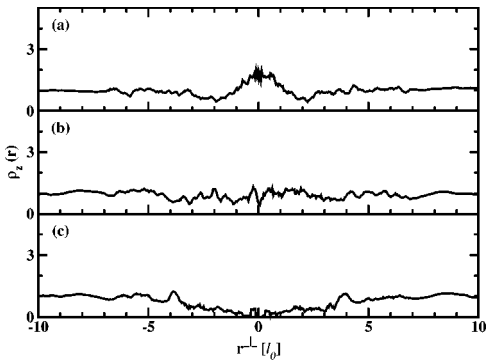

FIG. 11. Cross section of g_{ppz}, for 20 particles at $\nu=4/9$, along the arc perpendicular to the arc joining the fixed particle positions. (a)–(c) correspond to $d=1.0r_{pp}$, $0.5r_{pp}$, and $0.25r_{pp}$, respectively.

gether, the peak between them increases and narrows. This trend is most apparent in Figs. 4 and 5, which show the probability of finding a zero along an arc parallel and an arc transverse to the fixed particles (passing through the midpoint), respectively. We also see the emergence of prominent satellite peaks on either side of the two fixed particles, along the line joining the particles. The difference in the height of the central peak coming from the two orthogonal directions is strictly an artifact of the way a grid of bins is generated on the sphere.

To ascertain how this behavior evolves with filling factor, we next consider $\nu=3/7$ and 4/9. Figure 6 shows the d dependence of the probability of finding a zero near the fixed particles, for 21 particles at $\nu=3/7$. When $d=1.0r_{pp}$, we find behavior similar to that in the top panel of Fig. 3. This is to be expected, because in both cases the distance between the two fixed particles is a typical interparticle separation and the density of zeroes is essentially a sum of two uncorrelated densities. However, in the middle panel of Fig. 6, we see no significant increase in the probability of finding a zero halfway between the fixed particles as d is reduced from $1.0r_{pp}$ to $r_{pp}/2$, although the satellite peaks again appear. The difference in behavior, when compared to $\nu=2/5$, is further made apparent as d decreases to $r_{pp}/4$ in the bottom panel of Fig. 6 and in Figs. 7 and 8. The peak between the fixed particles vanishes; as do the satellite peaks. Instead of satellite peaks, a ring forms around the pair of fixed particles. A ring is to be expected in the limit $d=0$ at all filling factors, because then we have a single charge of $-2e$ at the origin. However, the central peak is much weaker at $\nu=3/7$ than at $\nu=2/5$ for any value of d.

The zeroes of the 20 particle state at $\nu=4/9$ behave in a manner similar to that at 3/7. Figure 9 and its cross-sections in Figs. 10 and 11 show the zero between the fixed particles being squeezed out as d decreases. In the bottom panel, when the central peak completely vanishes, a ring around the fixed particles emerges.

V. CONCLUSION

The zeroes of the FQHE states distribute themselves to maximize the interelectron separation. As discussed before, the zeroes of a particle in an incompressible quantum Hall liquid do not have a well defined physical meaning, especially the off-particle zeroes. They do not have a well defined charge or any other sharp quantum number associated with them. With that warning, we have investigated their structure for several filling factors. Our findings are as follows. (i) The zeroes form a liquid. (ii) There is a short-range repulsion between the zeroes. This also induces a repulsion between zeroes and particles, for the latter are the carriers of the Pauli zeroes. (For the special case of Laughlin's wave function, all zeroes sit on particles *not* because the zeroes are attracted to one another or to the particles, but because this is the most efficient way for *particles* to stay away from one another.) (iii) For some states, especially for $\nu=2/5$, there is an anomalously large probability of finding a zero right in the middle of a pair of *nearby* particles.

ACKNOWLEDGMENTS

This work was supported in part by the National Science Foundation under Grants No. DGE-9987589 (IGERT) and DMR-0240458. We are grateful to the High Performance Computing (HPC) Group led by V. Agarwala, J. Holmes, and J. Nucciarone, at the Penn State University ASET (Academic Services and Emerging Technologies) for assistance and computing time with the LION-XE cluster. The authors would also like to thank A.H. MacDonald, G. Murthy, M. Peterson, D. Pfannkuche, V. W. Scarola, and R. Shankar for valuable discussions.

*Current address: Theoretical Physics Department, Indian Association for the Cultivation of Science, Jadavpur, Kolkata 700 032, India.

[1] D. C. Tsui, H. L. Stormer, and A. C. Gossard, Phys. Rev. Lett. **48**, 1559 (1982).

[2] R. B. Laughlin, Phys. Rev. Lett. **50**, 1395 (1983).

[3] B. I. Halperin, Helv. Phys. Acta **556**, 75 (1983); Phys. Rev. Lett. **52**, 1583 (1984).

[4] J. K. Jain, Phys. Rev. Lett. **63**, 199 (1989); Phys. Rev. B **41**, 7653 (1990); Phys. Today **53**, 39 (2000).

[5] *Composite Fermions*, edited by Olle Heinonen (World Scientific, New York, 1998); *Perspectives in Quantum Hall Effects*, edited by S. Das Sarma and A. Pinczuk (Wiley, New York, 1997).

[6] D. P. Arovas, R. N. Bhatt, F. D. M. Haldane, P. B. Littlewood, and R. Rammal, Phys. Rev. Lett. **60**, 619 (1988).

[7] G. Fano, F. Ortolani, and E. Tosatti, Nuovo Cimento D **9**, 1337 (1987); S.-R. E. Yang, M.-C. Cha, and J. H. Han, Phys. Rev. B **62**, 8171 (2000); D. Pfannkuche and A. H. MacDonald (unpublished); K. Musaelin and R. J. Joynt, J. Phys.: Condens. Matter **8**, L105 (1996). Some studies of nodes in other contexts can be found in D. Bressanini, D. M. Ceperley, and P. J. Reynolds, in *Recent Progress in Quantum Monte Carlo* (World Scientific, Singapore, 2002); M. Hoffmann-Ostenhof, T. Hoffmann-Ostenhof, and H. Stremnitzer, Commun. Math. Phys. **163**, 185 (1994).

[8] G. Murthy and R. Shankar, cond-mat/0205326 (unpublished).

[9] F. D. M. Haldane, Phys. Rev. Lett. **51**, 605 (1983).

[10] T. T. Wu and C. N. Yang, Nucl. Phys. B **107**, 365 (1976).

[11] J. K. Jain and R. K. Kamilla, Int. J. Mod. Phys. B **11**, 2621 (1997); Phys. Rev. B **55**, R4895 (1997).

[12] D. Ceperley, G. V. Chester, and M. H. Kalos, Phys. Rev. B **16**, 3081 (1977).

[13] B. B. Mandelbrot, *The Fractal Geometry of Nature* (W.H. Freeman, San Francisco, 1983); J. Gleick, *Chaos: Making a New Science* (Penguin Books, New York, 1988).

[14] R. K. Kamilla, J. K. Jain, and S. M. Girvin, Phys. Rev. B **56**, 12 411 (1997).